IEEE Photonics Journal
An IEEE Photonics Society Publication

Open Access

Carrier Recombination Dynamics Investigations of Strain-Compensated InGaAsN Quantum Wells

Volume 4, Number 6, December 2012

Lifang Xu
Dinesh Patel
Carmen S. Menoni, Fellow, IEEE
Jon M. Pikal
Jeng-Ya Yeh
J. Y. T. Huang
Luke J. Mawst, Fellow, IEEE
Nelson Tansu, Senior Member, IEEE

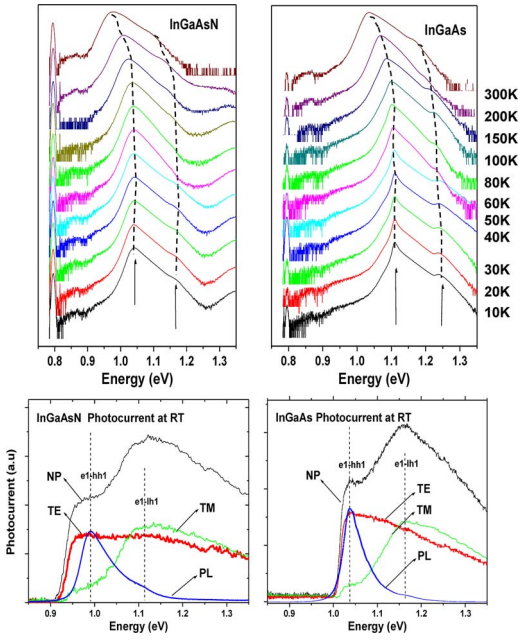

DOI: 10.1109/JPHOT.2012.2233465
1943-0655/$31.00 ©2012 IEEE

IEEE photonics SOCIETY

IEEE

Carrier Recombination Dynamics Investigations of Strain-Compensated InGaAsN Quantum Wells

Lifang Xu,[1] Dinesh Patel,[1] Carmen S. Menoni,[1] *Fellow, IEEE*, Jon M. Pikal,[2] Jeng-Ya Yeh,[3] J. Y. T. Huang,[3] Luke J. Mawst,[3] *Fellow, IEEE*, and Nelson Tansu,[4] *Senior Member, IEEE*

[1]Department of Electrical and Computer Engineering, Colorado State University, Fort Collins, CO 80523 USA
[2]Department of Electrical and Computer Engineering, University of Wyoming, Laramie, WY 82071 USA
[3]Reed Center for Photonics, Department of Electrical & Computer Engineering, University of Wisconsin-Madison, Madison, WI 53706 USA
[4]Center for Photonics and Nanoelectronics, Department of Electrical and Computer Engineering, Lehigh University, Bethlehem, PA 18015 USA

DOI: 10.1109/JPHOT.2012.2233465

Manuscript received October 24, 2012; accepted December 7, 2012. Date of publication December 11, 2012; date of current version December 24, 2012. This work was supported in part by the U.S. National Science Foundation under Grants ECCS 03134410 and ECCS 1028490 and in part by the Class of 1961 Professorship Fund (N.T.). Corresponding authors: N. Tansu, L. Xu, C. S. Menoni, and L. J. Mawst (e-mail: tansu@lehigh.edu; lifangxu417@yahoo.com; carmen.menoni@colostate.edu; mawst@engr.wisc.edu).

Abstract: The time evolution of the photoluminescence (PL) of 1300-nm emitting InGaAsN/GaAs/GaAsP strain-compensated single quantum well (QW) in the temperature range of $T = 10\ K - 300\ K$ is investigated. The PL spectra observed at the early stages of carrier recombination is dominated by two transitions. These two transitions are identified as the first quantized electron state to heavy-hole state (e1-hh1) and electron to light-hole state (e1-lh1) from the analysis of polarized photocurrent measurements in combination with $\boldsymbol{k} \cdot \boldsymbol{p}$ simulation of the band structure. At longer time delays, the dilute-nitride QW exhibits carrier localization at low temperatures and faster recombination time at higher temperatures. The PL dynamics characteristics observed in the InGaAsN QW are different from those measured from the InGaAs QW.

Index Terms: InGaAsN quantum well (QW), carrier recombination dynamics, carrier localization, 1.3-μm lasers, hole leakage.

1. Introduction

Dilute-nitride quantum wells (QWs) have been instrumental for realizing alloys with band gaps around 0.95 eV at room temperature suitable for enabling the uncooled telecom laser diodes emitting at ~1300 nm or beyond [1]–[10]. Significant progress has been accomplished in the field of dilute-nitride laser research during the past several years, particularly for achieving low-threshold dilute-nitride lasers [1]–[10], understanding and optimizing the high-temperature characteristics [11]–[17], understanding the recombination and gain characteristics [18]–[26], and investigating the high-speed performance [27]–[32] of the laser devices employing InGaAsN(Sb) QW active regions.

The use of strain-compensated InGaAsN QW with GaAsP barrier layers had resulted in very low threshold current density for laser devices emitting in the 1300-nm and 1400-nm spectral regimes [9], [10]. Though low-threshold current density devices have been realized for dilute-nitride lasers in

the 1300- to 1400-nm spectral regime, several key issues still remain of great interest to improve the temperature insensitivity of the threshold current at elevated temperature, as well as to improve the understanding of the effect of nitrogen incorporation into the InGaAsN QW on the optical response of the materials [33]–[36]. The improved insight into the physical origin of optical transitions and their dynamics is important, as this can shed light onto the understanding on the mechanism for achieving efficient optical emission. Although there were prior works on characterizations of emission lines in steady-state photoluminescence (PL) measurements [37]–[46], as of yet, no complete work has been accomplished on the study of corresponding recombination dynamics, which intends to provide input for new approaches toward the improvement of material quality.

In this paper, we have investigated the carrier recombination dynamics of InGaAs and InGaAsN QWs, particularly to understand the effect of the nitrogen incorporation on the recombination dynamics in the QW. Here, we performed a comprehensive study of the spectrally and temporarily resolved PL in the temperature range of $T = 10\ K - 300\ K$. The spectrally resolved PL, in addition to the e1-hh1 QW ground state, shows a higher energy emission line and is univocally characterized as the first quantized electron state to light-hole state (e1-lh1) transition. Time-resolved PL indicates that, at early stages after photoexcitation, carrier recombination takes place simultaneously for both light hole and heavy hole states. The simultaneous e1-hh1 and e1-lh1 transitions at the early stages of the photoexcitation are more severe in the InGaAsN QW. At longer time delays, the dilute-nitride QW exhibits carrier localization at low temperatures and faster recombination lifetime at higher temperatures. The behavior of the InGaAsN QW is in contrast to that measured in the InGaAs QW, of which the localization is absent at low temperature and the carrier lifetime increases with temperature as expected when radiative recombination dominates.

2. Experimental Works

Two strain-compensated InGaAs(N) single QW structures with 0 and 0.5% nitrogen content were investigated. Both samples were grown on a GaAs substrate by low-pressure (200 mbar) and low-temperature (530 °C) metal–organic chemical vapor deposition (MOCVD) [9]. The QW structure consists of a 6-nm $In_{0.4}Ga_{0.6}As_{0.995}N_{0.005}$ $(In_{0.4}Ga_{0.6}As)$ single-QW active layer sandwiched by 300-nm GaAs barrier. The lower and upper cladding layers are based on n-$Al_{0.85}Ga_{0.15}As$ and p-$In_{0.48}Ga_{0.52}P$, respectively. Partial strain compensation of the highly compressively strained QW was achieved by utilizing a 7.5-nm-thick $GaAs_{0.85}P_{0.15}$ tensile strain layers offset 10 nm from the QW. The threshold current densities of the 1300-nm emitting InGaAsN QW and 1200-nm emitting InGaAs QW broad area lasers were 220 A/cm^2 and 75 A/cm^2, respectively [2], [9].

For the spectrally resolved steady-state PL measurement, the QW samples were mounted on the cold finger of a closed-cycle Helium cryostat that allows varying the temperature from $T = 10$ K to $T = 300$ K. The PL was excited by a mode-locked Ti: sapphire laser-emitting 800-nm pulses with 100-fs duration and 82-MHz repetition rate. The fluence of the photoexcited carrier density at the sample was varied from 2×10^{10} cm^{-2} to 2×10^{12} cm^{-2} by attenuating the pump beam. For these excitation conditions, the photoexcited carriers were mainly created in the GaAs layer and then captured into the well; however, these photoexcited carrier densities are not high enough to cause significant band filling in the barrier region. The PL signal was detected by a nitrogen-cooled InGaAs detector through a spectrometer with a spectral resolution of 0.2 nm. The temporal evolution of the PL spectra was obtained using a luminescence upconversion technique. In this method, the Ti–sapphire pulses are divided into two trains of pulses. One pump beam is used to excite the sample, and the other beam travels through a delay line and is focused onto a 250 μm-thick beta-barium-borate (BBO) crystal coincident with the focused PL to generate the upconversion signal. The upconverted signal is spectrally resolved using a 0.3-m spectrometer and detected by a charge-coupled device (CCD). The temporal evolution is realized by changing the delay [47], and the time and spectral resolution of this process are mainly limited by the pulsed duration, $\sim$100 fs, and the spectral width, i.e., 9 meV, of the gating laser pulses.

To univocally identify the origin of the different PL transitions, polarization sensitive photocurrent (PC) measurements were performed at room temperature in InGaAs(N)/GaAs broad area lasers

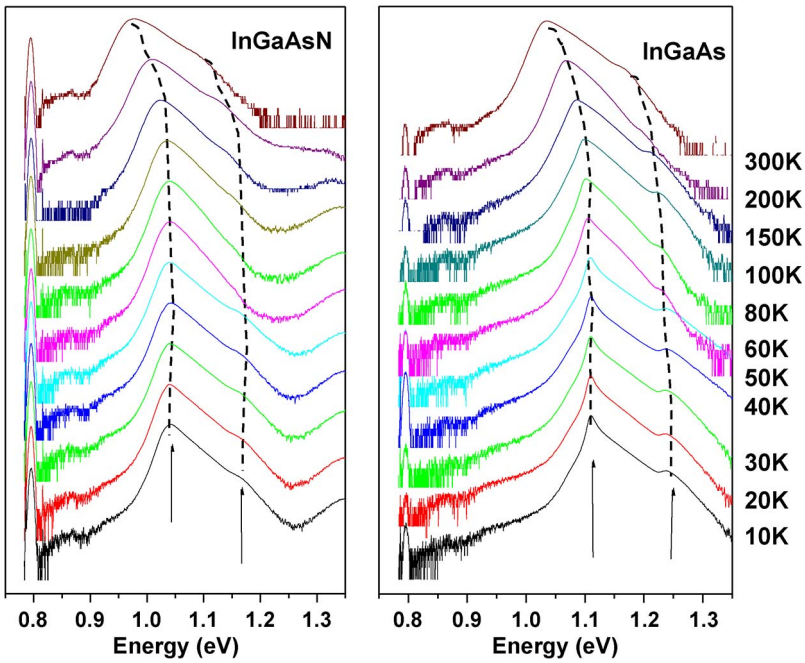

Fig. 1. Temperature dependence of time integrated PL spectrum of the InGaAsN QW and InGaAs QW measured at an excitation intensity of 1×10^{12} cm^{-2}, in logarithmic scale. The temperature range was varied from 10 K up to 300 K.

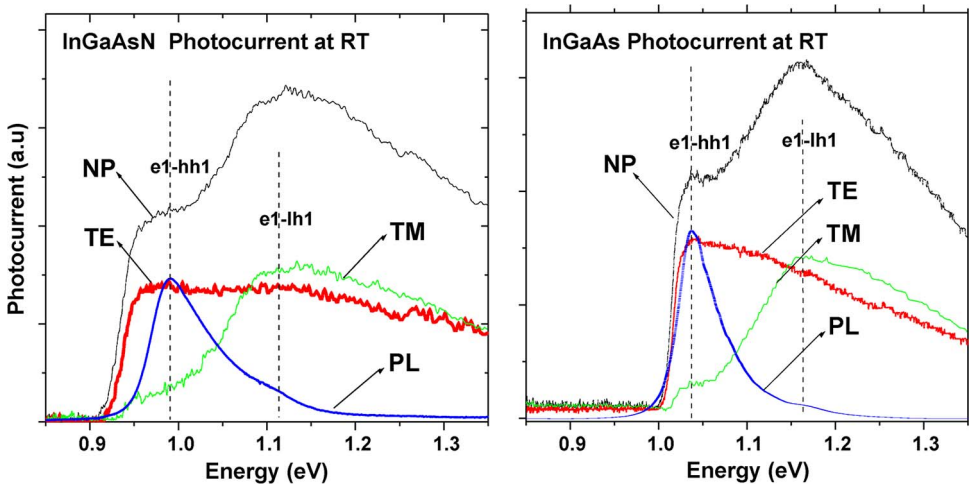

Fig. 2. Polarization dependent PC measurement at room temperature reveals the origin for each feature in PL.

identical to the structures used for PL measurements. The edge of the lasers was excited with a tungsten halogen lamp dispersed via a 0.75-m monochromator, and the current generated in the laser diode due to the facet illumination was recorded using lock-in technique.

3. Results and Discussion—Analysis

The normalized PL spectra of InGaAsN $(\mathrm{N} = 0,\ 0.5\%)$ is shown in Fig. 1 in the temperature range of $\mathrm{T} = 10\ \mathrm{K} - 300\ \mathrm{K}$. The photoexcited carrier density is 1×10^{12} cm^{-2}, which is close to the carrier density at threshold in device operation. The spectra contain two features, a more intense low

TABLE 1

Calculated quantized transition energies for InGaAsN QW and InGaAs QW by taking into consideration ten-band $\boldsymbol{k} \cdot \boldsymbol{p}$ model

QW – Barrier Designs	$E_{e1\text{-}hh1}$ (eV) $\lambda_{e1\text{-}hh1}$ (μm)	$E_{e1\text{-}lh1}$ (eV) $\lambda_{e1\text{-}lh1}$ (μm)
7-nm $In_{0.4}Ga_{0.6}As$ QWs / GaAs – $GaAs_{0.85}P_{0.15}$ Barriers	1.056 eV (1.174 μm)	1.205 eV (1.029 μm)
7-nm $In_{0.4}Ga_{0.6}As_{0.995}N_{0.005}$ QWs / GaAs – $GaAs_{0.85}P_{0.15}$ Barriers	1.016 eV (1.22 μm)	1.161 eV (1.068 μm)
7-nm $In_{0.4}Ga_{0.6}As_{0.992}N_{0.008}$ QWs / GaAs – $GaAs_{0.85}P_{0.15}$ Barriers	1.008 eV (1.23 μm)	1.148 eV (1.08 μm)

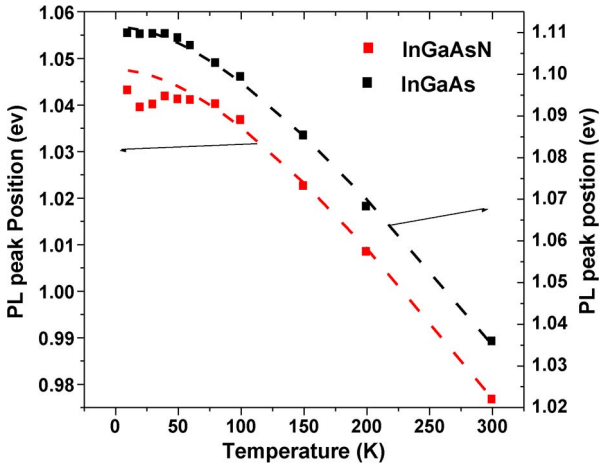

Fig. 3. Temperature dependence of PL peak energy positions for both InGaAsN QW and InGaAs QW samples. The dashed lines are the fitting results to the Varshni equation. The temperature was varied from 10 K up to 300 K.

energy peak, and a weaker higher energy peak. The lower energy peak corresponds to the QW band-gap transition, i.e., the first confined electron to first confined hole state (e1-hh1). In InGaAsN QW, the higher energy peak is separated from the lower energy peak by 120 (130) meV. The higher energy peak is assigned to the first confined electron to first confined light hole state (e1-lh1) transition, and this e1-lh1 transition was independently confirmed from the analysis of the polarization-dependent PC signal of InGaAsN QW and InGaAs QW samples. As shown in Fig. 2, the higher energy transition is predominantly TM-polarized, as expected from the selection rules governing optical transitions in QWs [48]. The weak presence of e1-hh1 transition in the TM-polarized PC spectra is likely due to symmetry breaking arising from the built-in junction field estimated to be $\sim$84 KV/cm.

The ten-band $\boldsymbol{k} \cdot \boldsymbol{p}$ calculations [49] that take into account the effect of the GaAsP strain-compensated layer provide further evidence on the origin of the higher energy peak being the e1-lh1 transition in InGaAs QW and InGaAsN QW, as shown in Table 1. Note that the ten-band $\boldsymbol{k} \cdot \boldsymbol{p}$ calculation [49] in Table 1 takes into consideration the GaAsP barrier layers in the analysis, and this model for III–V semiconductor QWs used here is similar to the approach described in [50] and [51]. These results agree with recent assignments from similar polarized edge-emission PL measurements [37]. In addition, our results also show that the e1-lh1 transitions clearly have 2-D properties despite the relatively low occupation of carriers in those lh1 states.

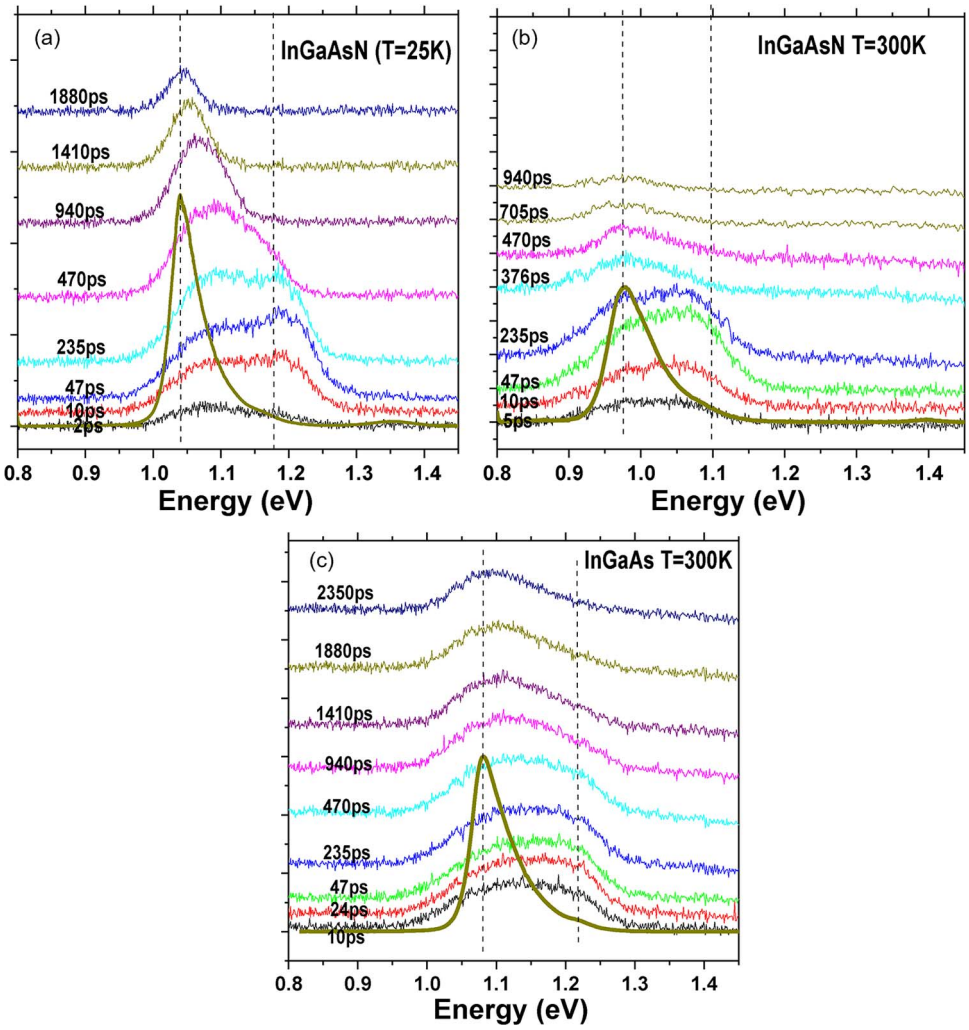

Fig. 4. Temporarily resolved PL spectra for the InGaAsN QW sample at different time delays for (a) T = 25 K and (b) T = 300 K, as well as (c) the comparison data of the InGaAs QW sample at T = 300 K [54]. The dashed lines in the plots represent the energy location of the e1-hh1 and e1-lh1 transitions observed in time integrated PL. The pump power into the sample was 30 mW.

We next focus in the temperature dependence of the PL peaks. As shown in Figs. 1 and 3, the e1-hh1 PL peaks in both InGaAsN QW and InGaAs QW have almost identical temperature behavior except below T $\sim$ 80 K. In InGaAs QW, the (e1-hh1) PL emission follows the well-known behavior described by the Varshni equation [52]. In InGaAsN QW, the Varshni-like behavior is observed above $\sim$80 K. In contrast, at lower temperatures, the S-shape behavior, already documented in the literature and associated with the trapping and detrapping of excitons to localized excitonic states [53], is observed.

The time-resolved spectra obtained from the upconversion experiments provided the means to investigate the carrier dynamics of the e1-hh1 and e1-lh1 transitions at early stages following photoexcitation [54]. A sequence of spectra taken at different delays for InGaAsN QW at T = 25 K and T = 300 K are shown in Fig. 4(a) and (b), while Fig. 4(c) shows the corresponding plot for InGaAs QW at T = 300 K for comparison purposes [54]. At T = 25 K, the e1-hh1 PL emission in InGaAsN QW [see Fig. 4(a)] shows a monotonous red shift of $\sim$30 meV taking place in the first $\sim$1.2 ns, which is further evidence of carrier localization that is also described by the S-shape variation of the band gap with temperature. This redshift decreases as temperature increases, and the redshift

characteristic is absent for all the measurements at room temperature [see Fig. 4(b)]. No localization effects are observed in InGaAs QW in the whole temperature range, which agree well with the findings shown in Fig. 3.

The dynamics of the PL spectra in Fig. 4(a) and (b) also showed that the higher energy e1-lh1 transition in InGaAsN QW is characterized by a shorter lifetime of $\sim$600 ps ($\sim$300 ps) versus $\sim$2000 ps ($\sim$700 ps) for the e1-hh1 transition at T = 25 K (T = 300 K), respectively. This finding is not surprising, as the light hole band in InGaAsN QW is barely confined, and this is affected by hole leakage to the barriers. Recent works [54] based on time-resolved two-color pump-probe transmission measurements had also shown a significant increase in thermionic carrier escape rate in InGaAsN-based QWs. In contrast, for InGaAs QW [see Fig. 4(c)], the e1-lh1 emission lifetime at room temperature is relatively long, i.e., $\sim$1500 ps, comparable with e1-hh1 transition lifetime of $\sim$2000 ps, which suggest a much better confinement of the light hole state in the InGaAs QW.

4. Summary

In summary, both e1-hh1 and e1-lh1 transitions in InGaAsN QW and InGaAs QW have been found to be populated with medium to high excitation intensity for measurements from T = 10 K – 300 K. The carrier dynamic process of the e1-lh1 transition is faster in InGaAsN QW, in comparison with its corresponding e1-h11 transition lifetime. In contrast, the transition lifetime of e1-lh1 for InGaAs QW is found as comparable with that of its corresponding e1-hh1 transition. Our paper also shows that the incorporation of nitrogen in the InGaAsN QW leads to carrier localization in the lowest energy state, which is strong at low temperature, persisting a long localized lifetime, and decreases as temperature increases. The improved understanding of the carrier recombination in the MOCVD-grown InGaAsN QW will be useful for further optimization of the threshold characteristics for these laser devices.

References

[1] D. A. Livshits, A. Y. Egorov, and H. Riechert, "8 W continuous wave operation of InGaAsN lasers at 1.3 μm," *Electron. Lett.*, vol. 36, no. 16, pp. 1381–1382, Aug. 2000.

[2] S. R. Bank, H. B. Yuen, M. A. Wistey, V. Lordi, H. P. Bae, and J. S. Harris, "Effects of growth temperature on the structural and optical properties of 1.55 μm GaInNAsSb quantum wells grown on GaAs," *Appl. Phys. Lett.*, vol. 87, no. 2, pp. 021908-1–021908-3, Jul. 2005.

[3] N. Tansu, J. Y. Yeh, and L. J. Mawst, "Physics and characteristics of 1200-nm InGaAs and 1300–1400 nm InGaAsN quantum-well lasers by metalorganic chemical vapor deposition," *J. Phys., Condens. Matter Phys.*, vol. 16, no. 31, pp. S3 277–S3 318, Aug. 2004.

[4] V. Gambin, W. Ha, M. Wistey, H. Yuen, S. R. Bank, S. M. Kim, and J. S. Harris, "GaInNAsSb for 1.3–1.6-μm-long wavelength lasers grown by molecular beam epitaxy," *IEEE J. Sel. Topics Quantum Electron.*, vol. 8, no. 4, pp. 795–800, Jul./Aug. 2002.

[5] S. R. Bank, M. A. Wistey, H. B. Yuen, L. L. Goddard, W. Ha, and J. S. Harris, Jr., "Low-threshold CW GaInNAsSb/GaAs laser at 1.49 μm," *Electron. Lett.*, vol. 39, no. 20, pp. 1445–1446, Oct. 2003.

[6] S. R. Bank, H. Bae, L. L. Goddard, H. B. Yuen, M. A. Wistey, R. Kudrawiecc, and J. S. Harris, "Recent progress on 1. 55-μm dilute-nitride lasers," *IEEE J. Quantum Electron.*, vol. 43, no. 9, pp. 773–785, Sep./Oct. 2007.

[7] C. Jin, H. Y. Liu, S. Y. Zhang, and M. Hopkinson, "Low-threshold 1.3-μm GaInNAs quantum-well lasers using quaternary-barrier structures," *IEEE Photon. Technol. Lett.*, vol. 20, no. 11, pp. 942–944, Jun. 2008.

[8] M. Guina, T. Leinonen, A. Harkonen, and M. Pessa, "High-power disk lasers based on dilute nitride heterostructures," *New J. Phys.*, vol. 11, no. 12, pp. 125019-1–125019-13, Dec. 2009.

[9] N. Tansu, N. J. Kirsch, and L. J. Mawst, "Low-threshold-current-density 1300-nm dilute-nitride quantum well lasers," *Appl. Phys. Lett.*, vol. 81, no. 14, pp. 2523–2525, Sep. 2002.

[10] J. Y. Yeh, N. Tansu, and L. J. Mawst, "Long wavelength MOCVD grown InGaAsN–GaAsN quantum well lasers emitting at 1.378–1.41 μm," *Electron. Lett.*, vol. 40, no. 12, pp. 739–741, Jun. 2004.

[11] S. R. Bank, L. L. Goddard, M. A. Wistey, H. B. Yuen, and J. S. Harris, "On the temperature sensitivity of 1.5-μm GaInNAsSb lasers," *IEEE J. Sel. Topics Quantum Electron.*, vol. 11, no. 5, pp. 1089–1098, Sep./Oct. 2005.

[12] L. L. Goddard, S. R. Bank, M. A. Wistey, H. B. Yuen, Z. Rao, and J. S. Harris, "Recombination, gain, band structure, efficiency, and reliability of 1.5-μm GaInNAsSb/GaAs lasers," *J. Appl. Phys.*, vol. 97, no. 8, pp. 083101-1–083101-15, Apr. 2005.

[13] R. Fehse, S. Tomic, A. R. Adams, S. J. Sweeney, E. P. O'Reilly, A. Andreev, and H. Riechert, "A quantitative study of radiative, auger, and defect related recombination processes in 1.3-μm GaInNAs-based quantum well lasers," *IEEE J. Sel. Topics Quantum Electron.*, vol. 8, no. 4, pp. 801–810, Jul./Aug. 2002.

[14] N. Tansu, J. Y. Yeh, and L. J. Mawst, "Experimental evidence of carrier leakage in InGaAsN quantum-well lasers," *Appl. Phys. Lett.*, vol. 83, no. 11, pp. 2112–2114, Sep. 2003.
[15] N. Tansu and L. J. Mawst, "Current injection efficiency of 1300-nm InGaAsN quantum-well lasers," *J. Appl. Phys.*, vol. 97, no. 5, pp. 054502-1–054502-18, Mar. 2005.
[16] J. Y. Yeh, L. J. Mawst, and N. Tansu, "The role of carrier transport on the current injection efficiency of InGaAsN quantum-well lasers," *IEEE Photon. Technol. Lett.*, vol. 17, no. 9, pp. 1779–1781, Sep. 2005.
[17] C. Y. Liu, S. F. Yoon, Q. Cao, C. Z. Tong, and Z. Z. Sun, "Comparative analysis of cavity length-dependent temperature sensitivity of GaInNAs quantum dot lasers and quantum well lasers," *Nanotechnol.*, vol. 17, no. 22, pp. 5627–5631, Nov. 2006.
[18] J. W. Ferguson, P. Blood, P. M. Smowton, H. Bae, T. Sarmiento, J. S. Harris, N. Tansu, and L. J. Mawst, "Optical gain in GaInNAs and GaInNAsSb quantum wells," *IEEE J. Quantum Electron.*, vol. 47, no. 6, pp. 870–877, Jun. 2011.
[19] S. B. Healy and E. P. O'Reilly, "Influence of electrostatic confinement on optical gain in GaInNAs quantum-well lasers," *IEEE J. Quantum Electron.*, vol. 42, no. 6, pp. 608–615, Jun. 2006.
[20] S. Tomic and E. P. O'Reilly, "Influence of confinement energy and band anticrossing effect on the electron effective mass in $Ga_{1-y}In_yN_xAs_{1-x}$ quantum wells," *Phys. Rev. B, Condens. Matter*, vol. 71, no. 23, pp. 233301-1–233301-4, Jun. 2005.
[21] M. M. Bajo, A. Hierro, J. M. Ulloa, J. Miguel-Sanchez, A. Guzman, B. Damilano, M. Hugues, M. Al-Khalfioui, J. Y. Duboz, and J. Massies, "Current spreading efficiency and Fermi level pinning in GaInNAs-GaAs quantum-well laser diodes," *IEEE J. Quantum Electron.*, vol. 46, no. 7, pp. 1058–1065, Jul. 2010.
[22] D. J. Palmer, P. M. Smowton, P. Blood, J. Y. Yeh, L. J. Mawst, and N. Tansu, "Effect of nitrogen on gain and efficiency in InGaAsN quantum-well lasers," *Appl. Phys. Lett.*, vol. 86, no. 7, pp. 071121-1–071121-3, Feb. 2005.
[23] H. Carrere, X. Marie, J. Barrau, and T. Amand, "Comparison of the optical gain of InGaAsN quantum-well lasers with GaAs or GaAsP barriers," *Appl. Phys. Lett.*, vol. 86, no. 7, pp. 071116-1–071116-3, Feb. 2005.
[24] A. Thranhardt, I. Kuznetsova, C. Schlichenmaier, S. W. Koch, L. Shterengas, G. Belenky, J. Y. Yeh, L. J. Mawst, N. Tansu, J. Hader, J. V. Moloney, and W. W. Chow, "Nitrogen incorporation effects on gain properties in GaInNAs lasers: Experiment and theory," *Appl. Phys. Lett.*, vol. 86, no. 20, pp. 201117-1–201117-3, May 2005.
[25] C. Schlichenmaier, A. Thranhardt, T. Meier, S. W. Koch, W. W. Chow, J. Hader, and J. V. Moloney, "Gain and carrier losses of (GaIn)(NAs) heterostructures in the 1300–1550 nm range," *Appl. Phys. Lett.*, vol. 87, no. 26, pp. 261109-1–261109-3, Dec. 2005.
[26] S. D. Wu, Y. G. Cao, S. Tomic, and F. Ishikawa, "The optical gain and radiative current density of GaInNAs/GaAs/AlGaAs separate confinement heterostructure quantum well lasers," *J. Appl. Phys.*, vol. 107, no. 1, pp. 013107-1–013107-6, Jan. 2010.
[27] G. Adolfsson, S. M. Wang, M. Sadeghi, J. Bengtsson, A. Larsson, J. J. Lim, V. Vilokkinen, and P. Melanen, "Effects of lateral diffusion on the temperature sensitivity of the threshold current for 1.3-μm double quantum-well GaInNAs-GaAs lasers," *IEEE J. Quantum Electron.*, vol. 44, no. 7, pp. 607–616, Jul. 2008.
[28] D. Gollub, S. Moses, and A. Forchel, "1.3μm double quantum well GaInNAs distributed feedback laser diode with 13.8 GHz small signal modulation bandwidth," *Electron. Lett.*, vol. 40, no. 19, pp. 1181–1182, Sep. 2004.
[29] J. S. Gustavsson, Y. Q. Wei, M. Sadeghi, S. M. Wang, and A. Larsson, "10 Gbit/s modulation of 1.3 μm GaInNAs lasers up to 110 °C," *Electron. Lett.*, vol. 42, no. 16, pp. 925–926, Aug. 2006.
[30] Y. Q. Wei, J. S. Gustavsson, A. Haglund, P. Modh, M. Sadeghi, S. M. Wang, and A. Larsson, "High-frequency modulation and bandwidth limitations of GaInNAs double-quantum-well lasers," *Appl. Phys. Lett.*, vol. 88, no. 5, pp. 051103-1–051103-3, Jan. 2006.
[31] O. Anton, L. Xu, D. Patel, C. S. Menoni, J. Y. Yeh, T. T. Van Roy, L. J. Mawst, and N. Tansu, "The intrinsic frequency response of 1.3-μm InGaAsN lasers in the range $T = 10\ ^\circ C - 80\ ^\circ C$," *IEEE Photon. Technol. Lett.*, vol. 18, no. 16, pp. 1774–1776, Aug. 2006.
[32] J. J. Lim, R. MacKenzie, S. Sujecki, M. Dumitrescu, S. M. Wang, M. Sadeghi, G. Adolfsson, A. Larsson, and E. C. Larkins, "Static and dynamic performance optimisation of a 1.3 μm GaInNAs ridge waveguide laser," *Opt. Quantum Electron.*, vol. 40, no. 14/15, pp. 1181–1186, Nov. 2008.
[33] O. Anton, D. Patel, C. S. Menoni, J. Y. Yeh, L. J. Mawst, J. M. Pikal, and N. Tansu, "Increased monomolecular recombination in MOCVD grown 1.3-μm InGaAsN–GaAsP–GaAs QW lasers from carrier lifetime measurements," *IEEE Photon. Technol. Lett.*, vol. 17, no. 5, pp. 954–955, May 2005.
[34] J. C. L. Yong, J. M. Rorison, M. Othman, H. D. Sun, M. D. Dawson, and K. A. Williams, "Simulation of gain and modulation bandwidths of 1300 nm RWG InGaAsN lasers," *Proc. Inst. Elect. Eng.—Optoelectron.*, vol. 150, no. 1, pp. 80–82, Feb. 2003.
[35] A. Albo, G. Bahir, and D. Fekete, "Improved hole confinement in GaInAsN–GaAsSbN thin double-layer quantum-well structure for telecom-wavelength lasers," *J. Appl. Phys.*, vol. 108, no. 9, pp. 093116-1–093116-6, Nov. 2010.
[36] J. Chamings, S. Ahmed, A. R. Adams, S. J. Sweeney, V. A. Odnoblyudov, C. W. Tu, B. Kunert, and W. Stolz, "Band anti-crossing and carrier recombination in dilute nitride phosphide based lasers and light emitting diodes," *Phys. Stat. Sol. (B)*, vol. 246, no. 3, pp. 527–531, Mar. 2009.
[37] H. D. Sun, A. H. Clark, S. Calvez, M. D. Dawson, N. Y. Qiu, J. M. Rorison, K. S. Kim, T. Kim, and Y. J. Park, "Spectroscopic characterization of 1.3μm GaInNAs quantum-well structures grown by metal–organic vapor phase epitaxy," *Appl. Phys. Lett.*, vol. 86, no. 9, pp. 092106-1–092106-3, Feb. 2005.
[38] N. J. Kim, Y. D. Jang, D. Lee, K. H. Park, W. G. Jeong, and J. W. Jang, "Reliable strain determination method for InGaAsN/GaAs quantum wells using a simple photoluminescence measurement," *Appl. Phys. Lett.*, vol. 83, no. 15, pp. 3114–3116, Oct. 2003.
[39] L. Xu, D. Patel, C. S. Menoni, J. Y. Yeh, L. J. Mawst, and N. Tansu, "Optical determination of electron effective-mass of strain compensated $In_{0.4}Ga_{0.6}As_{0.995}N_{0.005}/GaAs$ single quantum well," *Appl. Phys. Lett.*, vol. 89, no. 17, pp. 171112-1–171112-3, Oct. 2006.
[40] M. Hugues, B. Damilano, J.-Y. Duboz, and J. Massies, "Exciton dissociation and hole escape in the thermal photoluminescence quenching of (Ga,In)(N,As) quantum wells," *Phys. Rev. B, Condens. Matter*, vol. 75, no. 11, pp. 115337-1–115337-5, Mar. 2007.

[41] L. Geelhaar, M. Galluppi, R. Averbeck, G. Jaschke, and H. Riechert, "Annealing of InGaAsN quantum wells in hydrogen," *Appl. Phys. Lett.*, vol. 90, no. 7, pp. 071913-1–071913-3, Feb. 2007.
[42] J. Miguel-Sanchez, A. Guzman, and E. Munoz, "Role of N ions in the optical and morphological properties of InGaAsN quantum wells for 1.3–1.5 μm applications," *Appl. Phys. Lett.*, vol. 85, no. 11, pp. 1940–1942, Sep. 2007.
[43] J. Miguel-Sanchez, A. Guzman, J. M. Ulloa, A. Hierro, and E. Munoz, "Effect of nitrogen ions on the properties of InGaAsN quantum wells grown by plasma-assisted molecular beam epitaxy," *Proc. Inst. Elect. Eng.—Optoelectron.*, vol. 151, no. 5, pp. 305–308, Oct. 2004.
[44] C. S. Peng, J. Konttinen, H. F. Liu, and M. Pessa, "Blue shift in InGaAsN/GaAs quantum wells with different width," *Proc. Inst. Elect. Eng.—Optoelectron.*, vol. 151, no. 5, pp. 317–319, Oct. 2004.
[45] R. Kudrawiec, M. Gladysiewicz, J. Misiewicz, V. M. Korpijarvi, J. Pakarinen, J. Puustinen, P. Laukkanen, A. Laakso, M. Guina, M. Dumitrescu, and M. Pessa, "Contactless electroreflectance study of band bending in Be-doped GaInNAs/GaAs quantum wells: The origin of photoluminescence enhancement," *Appl. Phys. Lett.*, vol. 97, no. 2, pp. 021902-1–021902-3, Jul. 2010.
[46] I. Bosa, D. McPeake, and S. Fahy, "Effect of nitrogen interactions on photoluminescence linewidth broadening in dilute nitride semiconductors," *Phys. Rev. B, Condens. Matter*, vol. 78, no. 24, pp. 245206-1–245206-7, Dec. 2008.
[47] S. Haacke, R. A. Taylor, I. Bar-Joseph, M. J. S. P. Brasil, M. Hartig, and B. Deveaud, "Improving the signal-to-noise ratio of femtosecond luminescence upconversion by multichannel detection," *J. Opt. Soc. Amer. B, Opt. Phys.*, vol. 15, no. 4, pp. 1410–1417, Apr. 1998.
[48] S. L. Chuang, *Physics of Photonic Devices,* 2nd ed. New York: Wiley, 2009.
[49] I. Vurgaftman, J. R. Meyer, N. Tansu, and L. J. Mawst, "InP-based dilute-nitride mid-infrared Type-II 'W' quantum-well lasers," *J. Appl. Phys.*, vol. 96, no. 8, pp. 4653–4655, Oct. 2004.
[50] C. Y. P. Chao and S. L. Chuang, "Spin-orbit-coupling effects on the valence-band structure of strained semiconductor quantum wells," *Phys. Rev. B, Condens. Matter*, vol. 45, no. 7, pp. 4110–4122, Aug. 1992.
[51] H. Zhao, R. A. Arif, Y. K. Ee, and N. Tansu, "Self-consistent analysis of strain-compensated InGaN–AlGaN quantum wells for lasers and light-emitting diodes," *IEEE J. Quantum Electron.*, vol. 45, no. 1, pp. 66–78, Jan. 2009.
[52] K. P. O'Donnell and X. Chen, "Temperature dependence of semiconductor band-gaps," *Appl. Phys. Lett.*, vol. 58, no. 25, pp. 2924–2926, Jun. 1991.
[53] L. Grenouillet, C. Bru-Chevallier, G. Guillot, P. Gilet, P. Duvaut, C. Vannuffel, A. Million, and A. Chenevas-Paule, "Evidence of strong carrier localization below 100 K in a GaInNAs/GaAs single quantum well," *Appl. Phys. Lett.*, vol. 76, no. 16, pp. 2241–2243, Apr. 2000.
[54] L. F. Xu, D. Patel, C. S. Menoni, J. Y. Yeh, L. J. Mawst, and N. Tansu, "Experimental evidence of the impact of nitrogen on carrier capture and escape times in InGaAsN/GaAs single quantum well," *IEEE Photon. J.*, vol. 4, no. 6, pp. 2262–2271, Dec. 2012.